## CHEMISTRY

# A new route to synthesize aryl acetates from carbonylation of aryl methyl ethers

Qingqing Mei,[1,2] Youdi Yang,[1,2] Hangyu Liu,[1,2] Shaopeng Li,[1,2] Huizhen Liu,[1,2]* Buxing Han[1,2]*

Ether bond activation is very interesting because the synthesis of many valuable compounds involves conversion of ethers. Moreover, C–O bond cleavage is also very important for the transformation of biomass, especially lignin, which abundantly contains ether bonds. Developing efficient methods to activate aromatic ether bonds has attracted much attention. However, this is a challenge because of the inertness of aryl ether bonds. We proposed a new route to activate aryl methyl ether bonds and synthesize aryl acetates by carbonylation of aryl methyl ethers. The reaction could proceed over RhCl$_3$ in the presence of LiI and LiBF$_4$, and moderate to high yields of aryl acetates could be obtained from transformation of various aryl methyl ethers with different substituents. It was found that LiBF$_4$ could assist LiI to cleave aryl methyl ether bonds effectively. The reaction mechanism was proposed by a combination of experimental and theoretical studies.

## INTRODUCTION

The activation of the C–O bond and the transformation of ethers are significantly important from both scientific and practical viewpoints. For example, the conversion of dimethyl ether is a key issue in syngas chemistry (1). They are particularly crucial in lignin degradation and utilization because ether bonds are the main linkages in lignin (2). Biomass as a raw material to produce useful chemical compounds has attracted considerable interest (2–7), which can liberate us from our reliance on fossil resources and can also be considered as recycling of CO$_2$ by a combination of photosynthesis and chemical methods. Lignin is one of the main components of lignocellulosic biomass, which is a renewable carbon resource (8). Much attention has been paid to the depolymerization of lignin, and various useful products and platform molecules have been obtained, such as liquid fuels, alcohols, phenols, and aromatic ethers (9–13). There exist abundant structure units of aryl methyl ethers in lignin (2). Some aryl methyl ethers can be derived from lignin (for example, guaiacol and syringol), and some naturally exist in plants and can be directly extracted (for example, anisole and anethole). Aryl methyl ethers are widely used as lignin model compounds to study lignin transformation (2). With the extensive study of biomass valorization, conversion of aromatic ethers into more valuable chemicals is becoming particularly important and attracting increasing interest (14–16). For example, in our previous work, ketones were obtained by the hydrogenation and hydrolysis of aromatic ethers (17). However, because of the inertness of the aromatic ether bond, there remain great challenges to achieving highly efficient conversion of aromatic ethers into important compounds (18). Moreover, current methods to transform aryl methyl ethers mainly involve cleavage of the ether bonds, where the methoxyl/methyl groups usually result in side products. New approaches to direct utilization of the aryl-O-Me functional groups are highly desired.

Aryl acetates are value-added chemicals. For example, phenylacetate is an important compound that can be used as a solvent and as an intermediate for medicines and organic synthesis (19, 20). It has also been used in cancer detection (21, 22), and its rearrangement isomer, p-acetylphenol, can be used to cure cholecystitis and icterohepatitis. Different methods have been reported for preparing aryl acetates, and most of them involve acyl chloride or anhydride, which are risky reagents because of their high reactivity (23–26).

Here, we discovered that aryl acetates could be produced by the carbonylation of aryl methyl ethers (Fig. 1). It was found that the RhCl$_3$ catalyst in CH$_3$CN medium was highly efficient for the transformation of aryl methyl ethers into aryl acetates in the presence of LiI and LiBF$_4$ and that the yield of the desired product could be higher than 90%. In the experiments, we found that LiBF$_4$ could effectively promote the cleavage of ether bonds, which was further proved by theoretical calculations. As far as we know, this is the first report that shows the efficient synthesis of aryl acetates by carbonylation of aryl methyl ethers, which complements the current C–O activation/cleavage chemistry. In addition, the method is important for exploring new routes to biomass valorization, of which the transformation of aryl methyl ether units is a key issue.

## RESULTS

### Screen of catalysts and optimization of reaction conditions

We first screened the catalytic system and optimized the reaction conditions for carbonylation of anisole to phenylacetate (Table 1). The reaction proceeded smoothly in the presence of RhCl$_3$, LiI, and LiBF$_4$, and the yield could reach 90% (Table 1, entry 1). The reaction did not occur without LiI, and the amount of LiI had a significant influence on the reaction (Table 1, entries 1 to 4). Taking LiCl as the alternative to LiI, the reaction did not take place (Table 1, entry 5), suggesting the significance of I$^-$. LiBF$_4$ could greatly promote the reaction. The yield of phenylacetate was only 14% solely with RhCl$_3$ and LiI (Table 1, entry 6), and it increased to 90% with the aid of LiBF$_4$ (Table 1, entry 1). The amount of LiBF$_4$ had little effect on the reaction (Table 1, entries 1 and 7). If LiBF$_4$ was replaced with BF$_3$, then both the conversion of anisole and the yield of phenylacetate
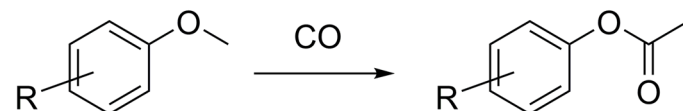


**Fig. 1. General scheme of the carbonylation reaction of aryl methyl ether to produce aryl acetate.**

[1]Beijing National Laboratory for Molecular Sciences, Chinese Academy of Sciences (CAS) Key Laboratory of Colloid, Interface, and Chemical Thermodynamics, CAS Research/Education Center for Excellence in Molecular Sciences, Institute of Chemistry, CAS, Beijing 100190, P. R. China. [2]School of Chemistry and Chemical Engineering, University of Chinese Academy of Sciences, Beijing 100049, P. R. China.
*Corresponding author. Email: liuhz@iccas.ac.cn (Huizhen Liu); hanbx@iccas.ac.cn (B.H.)

decreased sharply (Table 1, entry 8). The results were close to those without LiBF$_4$ (Table 1, entry 6), which suggested that LiBF$_4$ was crucial, whereas BF$_3$ almost had no effect on the reaction. The $^{19}$F nuclear magnetic resonance (NMR) spectrum (fig. S1) of the mixture after reaction showed only one peak at 148.88 parts per million, which was assigned to BF$_4^-$, and no signal of BF$_3$ was detected. This demonstrated that LiBF$_4$ was stable without decomposing into BF$_3$ in the reaction condition. When the lithium salts were changed to potassium salts, the reaction did not take place and the reactant remained untouched (Table 1, entry 9). This indicated that the acidity of Li$^+$ was also very important for the reaction. The pressure of CO considerably affected the yield, and the yield decreased to 63% when pressure decreased to 1 MPa (Table 1, entries 1 and 10). The yield of

phenylacetate reduced sharply to 9% as temperature decreased from 130° to 120°C (Table 1, entry 11). The effect of solvent was also checked (Table 1, entries 1 and 12 to 14). The yield of phenylacetate in a polar solvent was higher than that in an apolar solvent. In an apolar solvents, such as toluene and cyclohexane, the yields of phenylacetate were only 8 and 26%, respectively, whereas in a polar solvents, dimethyl sulfoxide (DMSO) gives a 59% yield of phenylacetate and CH$_3$CN was the best among the solvents used. Without RhCl$_3$, anisole could be almost completely converted to phenol, but no phenylacetate was produced (Table 1, entry 15). We also performed the reaction using Rh$_2$(CO)$_4$Cl$_2$, IrCl$_3$, PdCl$_2$, CoCl$_2$, and NiCl$_2$ as catalysts in the presence of LiI and LiBF$_4$ (Table 1, entries 16 to 20). The activity of Rh$_2$(CO)$_4$Cl$_2$ was the same as that of RhCl$_3$. It is known that [Rh(CO)$_2$I$_2$]$^-$ is the main active catalytic species in the carbonylation of CH$_3$I, and it can be derived from different Rh sources in the presence of CO and excess amount of iodine ions (27), which will be discussed in the "Reaction mechanism" section. Pd, Ir, Ni, and Co salts are also widely used in carbonylation reactions (28), but the activity of IrCl$_3$, PdCl$_2$, NiCl$_2$, and CoCl$_2$ was lower than that of RhCl$_3$ for the carbonylation of aryl methyl ethers (Table 1, entries 17 to 20). Although the conversion of anisole could reach 69 and 88% when using IrCl$_3$ and PdCl$_2$, the yields of phenylacetate were only 23 and 35%, respectively, and the main product was phenol. Only 2 and 7% yields of phenylacetate were achieved over NiCl$_2$ and CoCl$_2$ catalysts, and a large amount of phenol was also produced. It can be known from the results above that Rh species, BF$_4^-$, Li$^+$, and I$^-$ were indispensable for the excellent performance of the catalytic system. RhCl$_3$, LiI, and LiBF$_4$ cooperated very well in the reaction. The Rh species mainly catalyzed the carbonylation, whereas LiI acted as a cocatalyst in the carbonylation reaction and as a reagent for the cleavage of the ether bond, and LiBF$_4$ assisted LiI to cleave the ether bond. These are further discussed in detail in the following paragraphs.

## Role of LiBF$_4$

Among the several indispensable components in the catalytic system, the function of LiBF$_4$ is the most remarkable. It has not been reported to efficiently promote the cleavage of aryl alkyl ether bonds. We performed density functional theory (DFT) calculations to address the mechanism of the LiBF$_4$-promoted cleavage of the ether bond, focusing on the role of LiBF$_4$. The mechanism of the whole reaction is examined in the Discussion section. All the calculations were carried out with the M06-2x method combined with the TZVP (triple zeta valence polarized) all-electron basis set and the SDD (Stuttgart/Dresden) pseudopotential basis set (29–31), using the Gaussian 09 package (32), and the solvent effect was taken into account by the solvation model based on density (SMD) (33). First, we optimized the transition states of the cleavage of the ether bond of anisole by LiI alone without LiBF$_4$. It was found that LiI directly cleaves the ether bond through a four-membered ring transition state (Table 2, **TS-a**), and the Gibbs free-energy barrier is as high as 42.9 kcal/mol, which is too high, such that the reaction cannot take place under the experiment condition (130°C) through this path. With the help of two LiI via a six-membered ring (Table 2, **TS-b**), the energy barrier decreases to 37.6 kcal/mol. This is still a bit high for the reaction to take place smoothly at 130°C, which is consistent with the experimental result that the conversion of anisole was relatively low (26%) with solely LiI (Table 1, entry 6). Then, we investigated the situation in the presence of LiBF$_4$ and LiI, where LiBF$_4$ acts as a bridge to transfer the Li$^+$ cation from LiI to lithium phenolate. It was found that LiBF$_4$ can insert between the anisole and LiI of structure
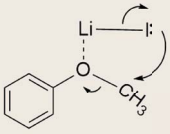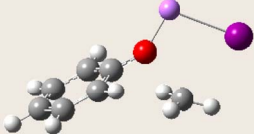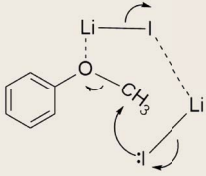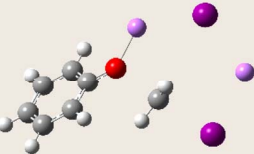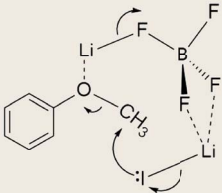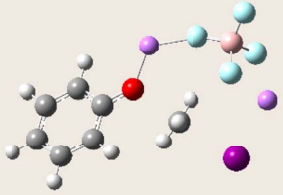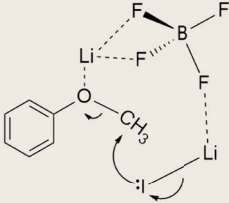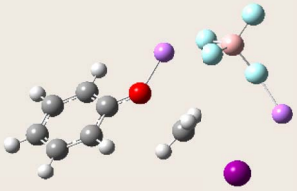
**Table 1. Optimization of reaction conditions for the carbonylation of anisole.** Reaction condition: **1a** (3 mmol), catalyst (1.5 mol%), and additives (0.66 eq LiI + 0.1 eq LiBF$_4$) in MeCN (1.5 ml); 12 hours; CO pressure, 2 MPa; 130°C.
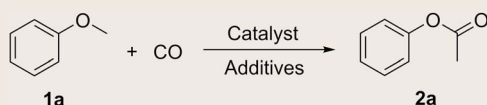


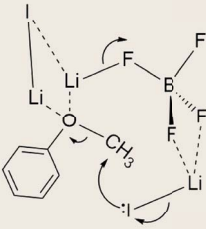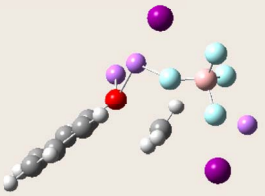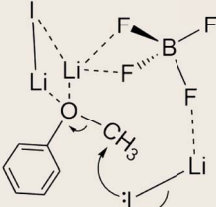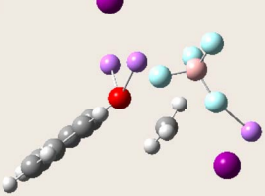| Entry | Catalyst | Additives | Solvent | Conv. (%)* | Yield (%)$^\dagger$ |
|---|---|---|---|---|---|
| 1 | RhCl$_3$ | LiI + LiBF$_4$ | MeCN | 100 | 90 |
| 2 | RhCl$_3$ | — | MeCN | 0 | 0 |
| 3 | RhCl$_3$ | LiBF$_4$ | MeCN | 0 | 0 |
| 4$^\ddagger$ | RhCl$_3$ | LiI + LiBF$_4$ | MeCN | 21 | 12 |
| 5 | RhCl$_3$ | LiCl + LiBF$_4$ | MeCN | 0 | 0 |
| 6 | RhCl$_3$ | LiI | MeCN | 26 | 14 |
| 7$^\S$ | RhCl$_3$ | LiI + LiBF$_4$ | MeCN | 100 | 89 |
| 8 | RhCl$_3$ | LiI + BF$_3$ | MeCN | 29 | 16 |
| 9 | RhCl$_3$ | KI + KBF$_4$ | MeCN | 0 | 0 |
| 10$^\P$ | RhCl$_3$ | LiI + LiBF$_4$ | MeCN | 90 | 63 |
| 11$^\|$ | RhCl$_3$ | LiI + LiBF$_4$ | MeCN | 33 | 9 |
| 12 | RhCl$_3$ | LiI + LiBF$_4$ | Toluene | 22 | 8 |
| 13 | RhCl$_3$ | LiI + LiBF$_4$ | Cyclohexane | 53 | 26 |
| 14 | RhCl$_3$ | LiI + LiBF$_4$ | DMSO | 90 | 59 |
| 15** | – | LiI + LiBF$_4$ | MeCN | 99 | 0 |
| 16 | Rh$_2$(CO)$_4$Cl$_2$ | LiI + LiBF$_4$ | MeCN | 100 | 90 |
| 17 | IrCl$_3$ | LiI + LiBF$_4$ | MeCN | 69 | 23 |
| 18 | PdCl$_2$ | LiI + LiBF$_4$ | MeCN | 88 | 35 |
| 19 | CoCl$_2$ | LiI + LiBF$_4$ | MeCN | 57 | 2 |
| 20 | NiCl$_2$ | LiI + LiBF$_4$ | MeCN | 47 | 7 |

*Conv., conversion.   $^\dagger$Yields were determined by $^1$H NMR analysis with tri-oxane as the internal standard.   $^\ddagger$LiI, 0.25 eq.   $^\S$LiBF$_4$, 0.3 eq.   $^\P$CO, 1 MPa.   $^\|$120°C.   **1 mmol anisole.

**Table 2. The pathways and structures of the transition states of the cleavage of the ether bond.** Structure optimization and free-energy calculation were conducted at the M06-2x/(SDD + TZVP) level. See Materials and Methods for more details. The Cartesian coordinates are listed in the Supplementary Materials.

| Pathway to the cleavage of ethers | Structure of the transition states | Barriers (kcal/mol) |
|---|---|---|
| **a** | **TS-a** | 42.9 |
| **b** | **TS-b** | 37.6 |
| **c** | **TS-c** | 35.1 |
| **d** | **TS-d** | 36.3 |
| **e** | **TS-e** | 27.0 |
| **f** | **TS-f** | 25.9 |

**a**, forming a seven-membered-ring transition state (**TS-c** and **TS-d**). There are two possible orientations of LiBF$_4$ (structures **c** and **d**), and the corresponding energy barriers are 35.1 and 36.3 kcal/mol, respectively, which are considerably lower than that of transition state **TS-a** and are very close to that of transition state **TS-b**. Inspired by this, we further considered the case of LiBF$_4$ inserted into structure **b**, and the energy barrier decreases to 27.0 kcal/mol (**TS-e**) and 25.9 kcal/mol (**TS-f**),

respectively, which are suitable for the ether bond cleavage at 130°C. In the process, the Li$^+$ cations of LiI and LiBF$_4$ interact with the O atom of anisole, which lengthens the O–CH$_3$ bond from 1.420 to 1.460 Å. Meanwhile, the natural population analysis (NPA) charge (34) of the methyl increases from 0.305 to 0.369, indicating that the C–O bond is weakened and that the methyl could be more easily nucleophilically attacked. On the other hand, the BF$_4^-$ anion interacts with another LiI

**Table 3. Substrate scope of the carbonylation of aryl methyl ethers.** Reaction condition: substrate (3 mmol), catalyst (1.5 mol%), and additives (0.66 eq LiI + 0.1 eq LiBF$_4$) in MeCN (1.5 ml); CO pressure, 2 MPa; 130°C. The reaction time for **1b**, **1c**, **1d**, and **1j** was 12 hours, and the reaction time for others was 18 hours.



| Entry | Substrates | Products | Yield[*] | Entry | Substrates | Products | Yield[*] |
|---|---|---|---|---|---|---|---|
| 1 | 1b | 2b | 87% | 2 | 1c | 2c | 93% |
| 3 | 1d | 2d | 92% | 4 | 1e | 2e | 88% |
| 5 | 1f | 2f | 89% | 6 | 1g | 2g | 91% |
| 7 | 1h | 2h | 89% | 8 | 1i | 2i | 84% |
| 9 | 1j | 2j | 80% | 10 | 1k | 2k | 79% |
| 11 | 1l | 2l | 81% | 12 | 1m | 2m | 84% |
| 13 | 1n | 2n | 81% | 14 | 1o | 2o | 54% |

[*]The yields of **2d**, **2h**, **2k**, and **2o** were determined by a gas chromatograph (GC), and others were determined by $^1$H NMR analysis with trioxane as the internal standard.

and makes it easier for $S_N2$ (bimolecular nucleophilic substitution) attack from the back of the methyl. Thus, the LiBF$_4$ salt can significantly promote the cleavage of the ether bond by LiI.

## Substrate scope

We also studied the performance of the catalytic system for the conversion of other aryl methyl ethers into corresponding aryl acetates. Table 3 shows the yields of the desired products for various substrates under optimized conditions, and most of them were greater than 80%. In general, the reactivity of the substrates with an electron-donating group was higher than that of the substrates with an electron-withdrawing group. For alkyl-substituted anisole (1b, 1c, and 1d), the yields of the corresponding acetates (2b, 2c, and 2d) were 87, 93, and 92% in 12 hours, respectively (Table 3, entries 1 to 3). For substituent groups with a weak electronic effect, such as –Cl, –NHCOCH$_3$, and –OCOCH$_3$, the reactivity of 1e, 1f, 1g, and 1h was similar to that of anisole, and the yield of the desired aryl acetates was about 90% (Table 3, entries 4 to 7). When the substituent group was stronger electron-withdrawing, the reactivity of the aryl methyl ether decreased slightly. For example, with the –CN (1i) or –F (1j) group on the aryl ring, the yields of 2i and 2j were 84 and 80%, respectively, which were a bit lower than that of 2a (Table 3, entries 8 and 9). Steric effects also had an obvious influence on the reaction. Substituents on the ortho position (1k and 1l) decreased the yield of the carbonylation products (Table 3, entries 10 and 11). Notably, the 5-O-4–type ether bond in 1k remained untouched, indicating the high selectivity of this catalytic system. The catalytic system was also active for methyl ether with a fused aromatic ring. For example, 2-methoxynaphthalene (1m) could be transformed into 2m with a yield of 84% in 18 hours. When the substrate had two –OCH$_3$ groups, the catalytic system was also active. For p-dimethoxybenzene (1n), the yield of 1,4-phenylene diacetate could reach 81% in 18 hours, and no 4-methoxyphenyl acetate was detected. For substrates with a competitive reaction site (1o), the yield of the desired aryl acetate (2o) was relatively low.

We also tested the reactivity of the lignin monomers guaiacol (1p) and syringol (1q). The reactions were conducted at 100°C for 48 hours,

and the results are shown in Fig. 2. Guaiacol was transformed to 48% yield of 2-hydroxyphenyl acetate (2p) and 10% yield of 1,2-phenylene diacetate (3p). The products for syringol were a bit complex, including 2-hydroxy-1,3-phenylene diacetate (2q), 3-hydroxy-1,2-phenylene diacetate (2q′), benzene-1,2,3-triyl triacetate (4q), dihydroxyphenyl acetates (3q and 3q′), and acetophenone derivates. The total yield of the main products, 2-hydroxy-1,3-phenylene diacetate (2q) and 3-hydroxy-1,2-phenylene diacetate (2q′), was 18%. The main reason for the low yield of desired products may be that the pyrogallol intermediates were very active and some unknown condensation reaction took place.

## DISCUSSION

### Reaction mechanism

We have demonstrated above that LiBF$_4$ could promote the reaction of LiI and aryl methyl ether to produce CH$_3$I. It is known that CH$_3$I is the active intermediate in the carbonylation reaction of methanol (28). In the presence of an Rh/I catalyst, CH$_3$I can react with CO to form acetyl iodide. The catalytic active species is the [Rh(CO)$_2$I$_2$]$^-$ anion, which can be derived in situ from different Rh sources (27). This may be the reason that RhCl$_3$ and Rh$_2$(CO)$_4$Cl$_2$ gave identical results (Table 1, entries 1 and 16). RhCl$_3$ can be reduced by CO to form [Rh(CO)$_2$I$_2$]$^-$ with an excess amount of iodide according to the equation in Fig. 3 (35). The reaction solution changed from dark reddish brown before the reaction to pale straw yellow after the reaction, which corresponded to the color of Rh(III) and [Rh(CO)$_2$I$_2$]$^-$, respectively (36). On the basis of the experimental results and the literature (27, 28), we proposed the possible reaction mechanism shown in Fig. 3. First, the ether bond was cleaved by LiI with the aid of LiBF$_4$, forming CH$_3$I and lithium phenolate. RhCl$_3$ was converted in situ to [Rh(CO)$_2$I$_2$]$^-$ as the catalytic active species, and the oxidative addition of CH$_3$I to it produced complex II. Then, an acetyl species (complex III) was formed via the fast immigration of methyl, and the leftover vacant coordination site was immediately saturated by a CO molecule. The
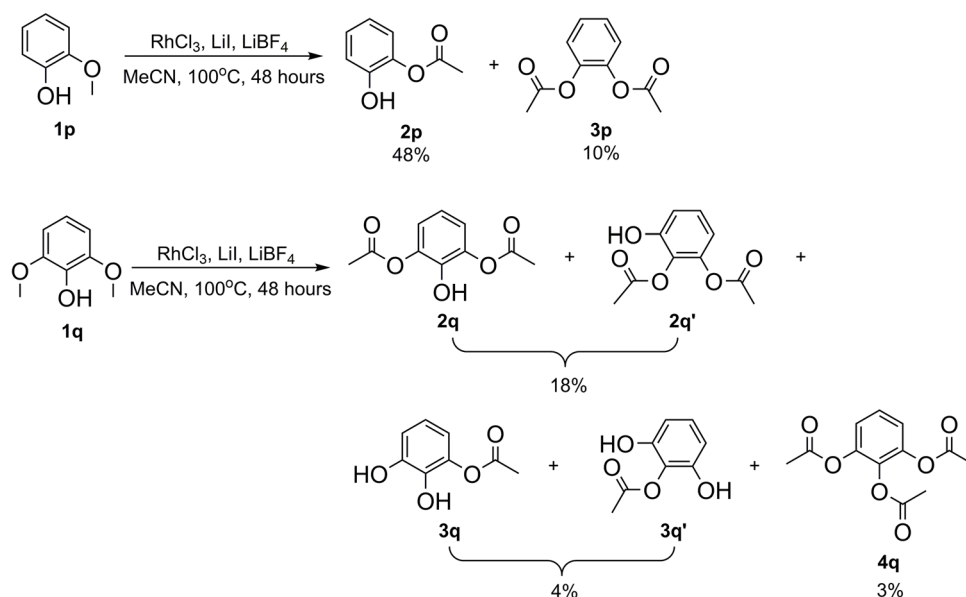
**Fig. 2. The carbonylation reaction of guaiacol (1p) and syringol (1q).** The yield of the products were determined by GC. The reaction conditions were the same as that in Table 3, except for the lower temperature (100°C) and the longer reaction time (48 hours).

$$RhCl_3 + 3CO + H_2O + 2I^- \longrightarrow [Rh(CO)_2I_2]^- + CO_2 + 2H^+ + 3Cl^-$$
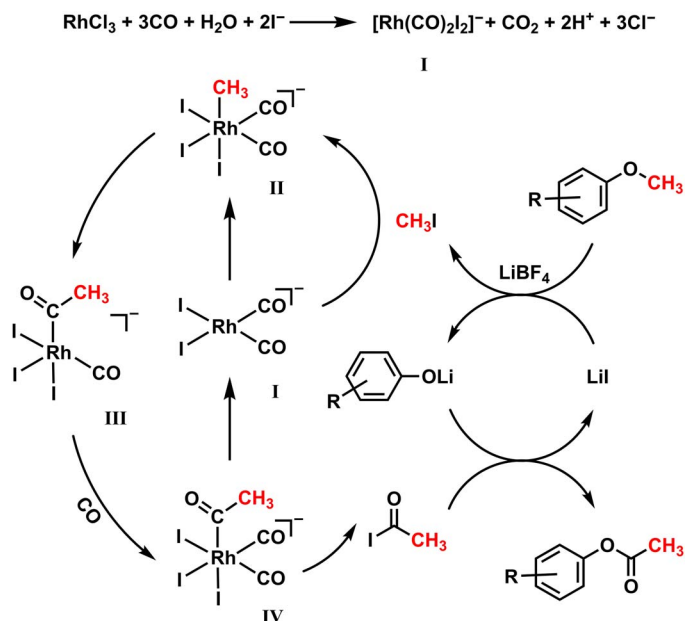
**Fig. 3. Possible reaction mechanism of the carbonylation of aryl methyl ethers.**

resulting complex **IV** decomposed and released an acetyl iodide molecule, regenerating the catalyst $[Rh(CO)_2I_2]^-$ (27). The total reaction of the Rh/I-catalyzed steps was the insertion of CO into the C–I bond of $CH_3I$ to produce acetyl iodide. Finally, lithium phenolate reacted with acetyl iodide and yielded the desired aryl acetate. Meanwhile, LiI was regenerated.

## Concluding remarks

In summary, a new method to produce aryl acetates was proposed, in which aryl methyl ethers and CO were used as the reactants. Various aryl methyl ethers could be efficiently carbonylated to the corresponding aryl acetate over the $RhCl_3$ catalyst with LiI and $LiBF_4$ as the cocatalysts in acetonitrile, and the yield could be higher than 90%. $RhCl_3$, LiI, and $LiBF_4$ were indispensable components and cooperated very well in the reaction. The Rh species mainly catalyzed the carbonylation, whereas LiI acted as a cocatalyst in the carbonylation reaction and as a reagent for the cleavage of the ether bond, and $LiBF_4$ assisted LiI to cleave the ether bond. DFT calculations showed that $LiBF_4$ could bridge two LiI ion pairs and reduce the energy barrier to cleave the C–O bond. This work provides a new method to activate aryl ether bonds and synthesize aryl acetates. Moreover, the finding is of importance for investigating efficient approaches to valorization of biomass or its derivatives because biomass contains abundant aryl ether bonds.

## MATERIALS AND METHODS
### Materials

Anisole (99%), 4-methylanisole (99%), 4-*tert*-butylanisole (98%), 3,5-difluoroanisole (98%), 4-bromo-2,6-dimethylanisole (99%), 3-chloroanisole (98%), 4-methoxybenzonitrile (99%), 1,4-dimethoxybenzene (98%), 4-chloroanisole (98%), 2-methoxynaphthalene (98%), and 1-methoxy-2,3,5-trimethylbenzene (97%) were provided by Beijing InnoChem Science & Technology Co. Ltd. Toluene (99%) was purchased from Sinopharm Chemical Reagent Co. Ltd. DMSO (99%), cyclohexane (99%), acetonitrile (99%), LiI (99%), $LiBF_4$ (98.5%),

$NiCl_2\cdot6H_2O$ (99%), and $CoCl_2\cdot6H_2O$ (99%) were purchased from J&K Scientific Ltd. $PdCl_2$ (>99%), $Rh_2(CO)_4Cl_2$ (>98%), $RhCl_3\cdot3H_2O$ (>98%), and $IrCl_3\cdot3H_2O$ (>98%) were purchased from Energy Chemical. All chemicals were used as received.

### Experimental procedure

The reaction was carried out in a Teflon-lined stainless steel reactor (15 ml) with a magnetic stirrer. In a typical experiment, the desired amount of aryl methyl ether, LiI, $LiBF_4$, $RuCl_3$, and anhydrous acetonitrile was loaded into the reactor. The reactor was sealed and purged with CO to remove the air. Then, CO was charged into the reactor to the desired pressure. The pressure was determined by a pressure transducer (FOXBORO/ICT, Model 93), which could be accurate to ±0.025 MPa. Then, the reactor was placed in an air bath of known temperature controlled by a proportional-integral-derivative temperature controller (model SX/A-1, Beijing SHUOYANG TIANCHENG Electronic Co. Ltd.). After the reaction, the reactor was placed in ice water, and the gas was released and collected in a gas sample bag. About 0.05 to 0.12 g of 1,3,5-trioxane as the internal standard was added to the liquid mixture and stirred for 5 min. For some of the samples, an appropriate amount of methanol was added to enhance the dissolution. After that, the mixture was centrifuged. The supernatant liquid was collected for qualitative analysis using gas chromatography–mass spectrometry (Agilent 7890B GC and 5977A Mass Selective Detector) and for quantitative analysis using $^1H$ NMR (Bruker Avance III 400 HD) in DMSO-$d_6$. The NMR spectra are shown in the Supplementary Materials. The peak of trioxane $[(CH_2O)_3, \delta 5.1]$ was used as the reference. The peaks of the protons in $-OCH_3(\delta 3.7)$ and $-OCOCH_3(\delta 2.2$ to $2.3)$ were used to determine the reactant conversion and the product yield, respectively. The peaks were chosen because they do not overlap with the signals of other protons of the reactant, product, and solvents. The baselines around these peaks were also flat for accurate integration. For **2d**, **2h**, **2k**, and **2o**, the peak of $-OCOCH_3$ was not appropriate for the quantitative analysis, so a GC (Agilent 6820) with a flame ionization detector was used instead. The gas sample was analyzed by using a GC (Agilent 4890D) equipped with a thermal conductivity detector and a packed column (Carbon molecular sieve TDX-01) using argon as the carrier gas. No gaseous product was generated in this work. The products were purified by silica-gel column chromatography using petroleum ether and ethyl acetate mixed solution as the eluent. The products were characterized by $^1H$ and $^{13}C$ NMR and high-resolution mass spectrometry (HRMS) with electron impact (EI) ionization (GTC Premier Spectrometer, Waters).

### Computational details

All the calculations were performed using Gaussian 09 software (34) with the M06-2x method (31). A def-TZVP basis set (32) was used for C, H, N, O, B, F, and Li, and the SDD (Stuttgart/Dresden) pseudo-potential and basis set (33) was used for iodine. Intrinsic reaction coordinate calculation was performed to confirm that a given transition state (solely imaginary frequency) connected a particular couple of consecutive minima (no imaginary frequency). The solvent effect of acetonitrile was taken into account by the SMD model (35). The NPA atomic charges (36) were calculated at the same level using the NBO 3.1 module (37) embedded in the Gaussian 09 package.

## SUPPLEMENTARY MATERIALS

Supplementary material for this article is available at http://advances.sciencemag.org/cgi/content/full/4/5/eaaq0266/DC1

section S1. $^{19}$F NMR spectrum of the reaction mixture after reaction

section S2. Quantity determination of the yield by $^{1}$H NMR

section S3. NMR and HRMS characterizations of the products

section S4. Cartesian coordinates of the transition states in Table 2

section S5. $^{1}$H and $^{13}$C NMR spectra of the products

fig. S1. $^{19}$F NMR spectrum of the reaction mixture after reaction under the conditions of entry 1 of Table 1.

table S1. Coordinates of transition state **TS-a**.

table S2. Coordinates of transition state **TS-b**.

table S3. Coordinates of transition state **TS-c**.

table S4. Coordinates of transition state **TS-d**.

table S5. Coordinates of transition state **TS-e**.

table S6. Coordinates of transition state **TS-f**.

# REFERENCES AND NOTES

1. P. Cheung, A. Bhan, G. J. Sunley, E. Iglesia, Selective carbonylation of dimethyl ether to methyl acetate catalyzed by acidic zeolites. *Angew. Chem. Int. Ed.* **45**, 1617–1620 (2006).

2. J. Zakzeski, P. C. A. Bruijnincx, A. L. Jongerius, B. M. Weckhuysen, The catalytic valorization of lignin for the production of renewable chemicals. *Chem. Rev.* **110**, 3552–3599 (2010).

3. C. O. Tuck, E. Pérez, I. T. Horváth, R. A. Sheldon, M. Poliakoff, Valorization of biomass: Deriving more value from waste. *Science* **337**, 695–699 (2012).

4. L. Shuai, M. T. Amiri, Y. M. Questell-Santiago, F. Héroguel, Y. Li, H. Kim, R. Meilan, C. Chapple, J. Ralph, J. S. Luterbacher, Formaldehyde stabilization facilitates lignin monomer production during biomass depolymerization. *Science* **354**, 329–333 (2016).

5. P. J. Deuss, M. Scott, F. Tran, N. J. Westwood, J. G. de Vries, K. Barta, Aromatic monomers by in situ conversion of reactive intermediates in the acid-catalyzed depolymerization of lignin. *J. Am. Chem. Soc.* **137**, 7456–7467 (2015).

6. B. M. Upton, A. M. Kasko, Strategies for the conversion of lignin to high-value polymeric materials: Review and perspective. *Chem. Rev.* **116**, 2275–2306 (2016).

7. C. Li, X. Zhao, A. Wang, G. W. Huber, T. Zhang, Catalytic transformation of lignin for the production of chemicals and fuels. *Chem. Rev.* **115**, 11559–11624 (2015).

8. T. E. Amidon, S. Liu, Water-based woody biorefinery. *Biotechnol. Adv.* **27**, 542–550 (2009).

9. A. Rahimi, A. Ulbrich, J. J. Coon, S. S. Stahl, Formic-acid-induced depolymerization of oxidized lignin to aromatics. *Nature* **515**, 249–252 (2014).

10. S. Stiefel, A. Schmitz, J. Peters, D. Di Marino, M. Wessling, An integrated electrochemical process to convert lignin to value-added products under mild conditions. *Green Chem.* **18**, 4999–5007 (2016).

11. C. S. Lancefield, O. S. Ojo, F. Tran, N. J. Westwood, Isolation of functionalized phenolic monomers through selective oxidation and C–O bond cleavage of the β-O-4 linkages in lignin. *Angew. Chem. Int. Ed.* **54**, 258–262 (2015).

12. Q. Song, F. Wang, J. Cai, Y. Wang, J. Zhang, W. Yu, J. Xu, Lignin depolymerization (LDP) in alcohol over nickel-based catalysts via a fragmentation-hydrogenolysis process. *Energ. Environ. Sci.* **6**, 994–1007 (2013).

13. A. K. Deepa, P. L. Dhepe, Lignin depolymerization into aromatic monomers over solid acid catalysts. *ACS Catal.* **5**, 365–379 (2015).

14. F. Gao, J. D. Webb, J. F. Hartwig, Chemo- and regioselective hydrogenolysis of diaryl ether C–O bonds by a robust heterogeneous Ni/C catalyst: Applications to the cleavage of complex lignin-related fragments. *Angew. Chem. Int. Ed.* **55**, 1474–1478 (2016).

15. A. G. Sergeev, J. F. Hartwig, Selective, nickel-catalyzed hydrogenolysis of aryl ethers. *Science* **332**, 439–443 (2011).

16. S. K. Boovanahalli, D. W. Kim, D. Y. Chi, Application of ionic liquid halide nucleophilicity for the cleavage of ethers: A green protocol for the regeneration of phenols from ethers. *J. Org. Chem.* **69**, 3340–3344 (2004).

17. Q. Meng, M. Hou, H. Liu, J. Song, B. Han, Synthesis of ketones from biomass-derived feedstock. *Nat. Commun.* **8**, 14190 (2017).

18. M. V. Bhatt, S. U. Kulkarni, Cleavage of ethers. *Synthesis* **1983**, 249–282 (1983).

19. R. van Putten, E. A. Uslamin, M. Garbe, C. Liu, A. Gonzalez-de-Castro, M. Lutz, K. Junge, E. J. M. Hensen, M. Beller, L. Lefort, E. A. Pidko, Non-pincer-type manganese complexes as efficient catalysts for the hydrogenation of esters. *Angew. Chem. Int. Ed.* **56**, 7531–7534 (2017).

20. T. K. Salvador, C. H. Arnett, S. Kundu, N. G. Sapiezynski, J. A. Bertke, M. Raghibi Boroujeni, T. H. Warren, Copper catalyzed sp$^3$ C–H etherification with acyl protected phenols. *J. Am. Chem. Soc.* **138**, 16580–16583 (2016).

21. D. Samid, Z. Ram, W. R. Hudgins, S. Shack, L. Liu, S. Walbridge, E. H. Oldfield, C. E. Myers, Selective activity of phenylacetate against malignant gliomas: Resemblance to fetal brain damage in phenylketonuria. *Cancer Res.* **54**, 891–895 (1994).

22. S. M. Chang, J. G. Kuhn, H. I. Robins, S. C. Schold, A. M. Spence, M. S. Berger, M. P. Mehta, M. E. Bozik, I. Pollack, D. Schiff, M. Gilbert, C. Rankin, M. D. Prados, Phase II study

23. of phenylacetate in patients with recurrent malignant glioma: A North American Brain Tumor Consortium Report. *J. Clin. Oncol.* **17**, 984–990 (1999).

23. A. K. Cook, M. S. Sanford, Mechanism of the palladium-catalyzed arene C–H acetoxylation: A comparison of catalysts and ligand effects. *J. Am. Chem. Soc.* **137**, 3109–3118 (2015).

24. M. H. Emmert, J. B. Gary, J. M. Villalobos, M. S. Sanford, Platinum and palladium complexes containing cationic ligands as catalysts for arene H/D exchange and oxidation. *Angew. Chem. Int. Ed.* **49**, 5884–5886 (2010).

25. M. H. Emmert, A. K. Cook, Y. J. Xie, M. S. Sanford, Remarkably high reactivity of Pd(OAc)$_2$/pyridine catalysts: Nondirected C–H oxygenation of arenes. *Angew. Chem. Int. Ed.* **50**, 9409–9412 (2011).

26. F. Rajabi, R. Luque, Solventless acetylation of alcohols and phenols catalyzed by supported iron oxide nanoparticles. *Catal. Commun.* **45**, 129–132 (2014).

27. D. J. Drury, Homogeneous catalysis using iodide-promoted rhodium catalysts, in *Aspects of Homogeneous Catalysis: A Series of Advances*, R. Ugo, Ed. (Springer Netherlands, 1984), pp. 197–216.

28. M. Beller, *Catalytic Carbonylation Reactions* (Springer Berlin Heidelberg, 2006).

29. Y. Zhao, D. G. Truhlar, The M06 suite of density functionals for main group thermochemistry, thermochemical kinetics, noncovalent interactions, excited states, and transition elements: Two new functionals and systematic testing of four M06-class functionals and 12 other functionals. *Theor. Chem. Acc.* **120**, 215–241 (2008).

30. A. Schäfer, C. Huber, R. Ahlrichs, Fully optimized contracted Gaussian basis sets of triple zeta valence quality for atoms Li to Kr. *J. Chem. Phys.* **100**, 5829–5835 (1994).

31. D. Andrae, U. Häußermann, M. Dolg, H. Stoll, H. Preuß, Energy-adjusted ab initio pseudopotentials for the second and third row transition elements. *Theor. Chim. Acta* **77**, 123–141 (1990).

32. M. J. Frisch, G. W. Trucks, H. B. Schlegel, G. E. Scuseria, M. A. Robb, J. R. Cheeseman, G. Scalmani, V. Barone, B. Mennucci, G. A. Petersson, H. Nakatsuji, M. Caricato, X. Li, H. P. Hratchian, A. F. Izmaylov, J. Bloino, G. Zheng, J. L. Sonnenberg, M. Hada, M. Ehara, K. Toyota, R. Fukuda, J. Hasegawa, M. Ishida, T. Nakajima, Y. Honda, O. Kitao, H. Nakai, T. Vreven, J. A. Montgomery Jr., J. E. Peralta, F. Ogliaro, M. Bearpark, J. J. Heyd, E. Brothers, K. N. Kudin, V. N. Staroverov, R. Kobayashi, J. Normand, K. Raghavachari, A. Rendell, J. C. Burant, S. S. Iyengar, J. Tomasi, M. Cossi, N. Rega, J. M. Millam, M. Klene, J. E. Knox, J. B. Cross, V. Bakken, C. Adamo, J. Jaramillo, R. Gomperts, R. E. Stratmann, O. Yazyev, A. J. Austin, R. Cammi, C. Pomelli, J. W. Ochterski, R. L. Martin, K. Morokuma, V. G. Zakrzewski, G. A. Voth, P. Salvador, J. J. Dannenberg, S. Dapprich, A. D. Daniels, Ö. Farkas, J. B. Foresman, J. V. Ortiz, J. Cioslowski, D. J. Fox, Gaussian software, version 09 revision D.01 (Gaussian Inc., 2009).

33. A. V. Marenich, C. J. Cramer, D. G. Truhlar, Universal solvation model based on solute electron density and on a continuum model of the solvent defined by the bulk dielectric constant and atomic surface tensions. *J. Phys. Chem. B* **113**, 6378–6396 (2009).

34. A. E. Reed, R. B. Weinstock, F. Weinhold, Natural population analysis. *J. Chem. Phys.* **83**, 735–746 (1985).

35. D. Forster, On the mechanism of a rhodium-complex-catalyzed carbonylation of methanol to acetic acid. *J. Am. Chem. Soc.* **98**, 846–848 (1976).

36. D. J. Drury, M. J. Green, D. J. M. Ray, A. J. Stevenson, Homogeneous catalysis of the hydrogenation of methanol using iodide-promoted rhodium catalysts. *J. Organomet. Chem.* **236**, C23–C27 (1982).

37. NBO Version 3.1, E. D. Glendening, A. E. Reed, J. E. Carpenter, F. Weinhold (2003).

# Science Advances

## A new route to synthesize aryl acetates from carbonylation of aryl methyl ethers

Qingqing Mei, Youdi Yang, Hangyu Liu, Shaopeng Li, Huizhen Liu and Buxing Han

| | |
|---|---|
| **ARTICLE TOOLS** | http://advances.sciencemag.org/content/4/5/eaaq0266 |
| **SUPPLEMENTARY MATERIALS** | http://advances.sciencemag.org/content/suppl/2018/05/14/4.5.eaaq0266.DC1 |
| **REFERENCES** | This article cites 33 articles, 5 of which you can access for free http://advances.sciencemag.org/content/4/5/eaaq0266#BIBL |
| **PERMISSIONS** | http://www.sciencemag.org/help/reprints-and-permissions |

Use of this article is subject to the Terms of Service